Static and dynamic magnetic properties of coupled spin-1/2 antiferromagnetic chains

2000 J. Phys.: Condens. Matter 12 8191

(http://iopscience.iop.org/0953-8984/12/37/316)

J. Phys.: Condens. Matter **12** (2000) 8191–8207. Printed in the UK PII: S0953-8984(00)14826-X

Static and dynamic magnetic properties of coupled spin-1/2 antiferromagnetic chains

S S Aplesnin†

L V Kirensky Institute of Physics, Siberian Branch of the Russian Academy of Science, Krasnoyarsk, 660036, Russia

E-mail: apl@iph.krasn.ru

Received 16 June 2000

Abstract. Calculations of the thermodynamic quantities, and the spectra of spinons, triplet excitations, and two-particle spin-singlet ($\Delta S^z = 0, \pm 1$) excitations for a weakly coupled antiferromagnetic $S = 1/2$ spin chain are made using a mean-field approximation for the interchain couplings (J_2) by the quantum Monte Carlo method. The mass gaps in these excitation spectra are estimated as functions of the interchain coupling. The critical field H_c, and the temperatures at which the spinon and singlet gaps close (T_1 and T_2, respectively) are obtained. Some peculiarities of the staggered magnetization, the specific heat, and the spin–spin correlation function are found at $T_1 = 0.9J_2$, $T_2 = 1.5J_2$, $H_c = 3.8J_2$, as determined by linear function fitting for $J_2/J_1 < 0.15$. The intrachain and interchain couplings, and the staggered magnetization for $KCuF_3$, Sr_2CuO_3, and Ca_2CuO_3 are estimated, and mass gaps are predicted to exist in the spectra of the spinons and the singlet two-particle excitations.

1. Indroduction

One-dimensional spin systems with antiferromagnetic interactions have received considerable attention because of their pronounced mechanical effects. One interesting question is that of whether the ground state is ordered or disordered when interactions between the chains are introduced. Previously, it was proposed that there is a nonzero critical coupling ratio, below which the system retains a singlet ground state [1]. Numerical studies of the Heisenberg model suggested a vanishing critical coupling ratio and that infinitesimally small interchain couplings should exhibit Néel order [2]. The best agreement with experiments, in contrast to the case for spin-wave theory [3], is obtained using a mean-field approximation for the interchain coupling [4–6]. There have been treatments of a one-dimensional antiferromagnet in an effective staggered field $h = (-1)^i\, 4J_2\langle S_i^z\rangle$, with the order parameter $\langle S_i^z\rangle$ determined by minimizing the energy. For more accurate simulation of static quantities, one needs to make allowance for local fluctuations of the staggered field.

Quasi-one-dimensional quantum magnets exhibit several kinds of the elementary excitation in the magnetic ordered state. For example, the exact solution for the antiferromagnetic spin-1/2 Heisenberg chain shows that the low-lying excitations are spin-1/2 objects [7] (now called spinons), quite different from standard spin waves. The interchain coupling induces a mass gap for the spinon excitations; this can be derived from the fermionic model, and in the continuum limit is $\Delta = 6.175J_2$ [5]. However, a single-mode approximation

† Fax: 07 3912 438923.

for a one-dimensional antiferromagnet in an effective staggered field [5] gives a massless spin-wave mode along the chain. This result is based on the following assumptions: the magnitude of the staggered magnetization is independent of the orientation of the staggered field, and the operators $S^+(q_z \simeq \pi)$ and $S^+(q_z \simeq 0)$ are a Lorentz scalar and vector, respectively; consequently the dynamical susceptibility $\chi(\pi + q, w)$ is a function of $w^2 - v^2q^2$ only.

In this paper we show that an infinitesimally small longitudinal external field breaks the spin-rotational invariance of the staggered magnetization and the staggered field induces a gap in the triplet excitation spectrum, which is not symmetrical with respect to the midpoint of the band ($q = \pi/2$). We estimate the two-particle excitation spectrum with respect to the interchain interaction, and predict new mass gaps for the low-dimensional magnets $KCuF_3$ [8,9], Sr_2CuO_3, and Ca_2CuO_3 [10,11]. The static and dynamic properties of a magnet can be investigated using various Monte Carlo (MC) schemes. The Green-function MC or, more generally, the projection-operator method is applicable at zero temperature ($T = 0$) only, and the final result depends on the trial wave function. For $T > 0$, the MC method is based on the Suzuki–Trotter discretization of imaginary time, and the loop-cluster-update algorithm may be used. In this scheme, a D-dimensional quantum system is transformed into the corresponding $(D + 1)$-dimensional classical system, with the accuracy of the exponential operator decomposition $\sim 1/(mT/J)^2$, where m is the size of the complementary dimension. The decrease of the interchain coupling ($\lambda = J_2/J_1$) leads to an increase in value of m that is $\sim 1/\lambda$, because the Néel temperature is a function of T_N which is $\sim\lambda$ [5]. According to scaling theory, the correlation radius of the spinon interaction is inversely proportional to the gap in the excitation spectrum, $\xi \sim 1/\Delta \sim 1/\lambda$, $L \geqslant 4\xi$ [5]. So we can give an estimate for the lattice size $N = L^D 2^D m$: $N \sim 2^D/\lambda^{D+1}$, and for $\lambda = 0.05$, $N = 1280\,000$ sites are required to calculate the spinon excitation spectrum at the various temperatures and fields. Therefore, we are compelled to use a combination of two methods: the Monte Carlo method and the mean-field approximation.

2. Model and method

We shall consider the Heisenberg model with negative interactions between nearest neighbours with $S = 1/2$ directed along an external-field OZ-direction. The Hamiltonian takes the form

$$H = -J_1 \sum_{i,j} \boldsymbol{S}_{i,j} \cdot \boldsymbol{S}_{i+1,j} - J_2 \sum_{i,j,\delta} \boldsymbol{S}_{i,j} \cdot \boldsymbol{S}_{i,j+\delta} - \sum_i H^z S_i^z \tag{1}$$

where $J_1 < 0$, $J_2 < 0$ are the intrachain and interchain couplings, $\lambda = J_2/J_1$, H^z is an external magnetic field, and δ is summed over the nearest neighbours in the transverse directions ($z = 4$). Now we transform the Hamiltonian (1) into an effective single-chain problem using a mean-field treatment of the interchain coupling [5,6]. The Hamiltonian now takes the form

$$H_1 = -J_1 \sum_{i=1}^{L} \boldsymbol{S}_i \cdot \boldsymbol{S}_{i+1} - \sum_{i=1}^{L} h_i S_i^z - \sum_{i=1}^{L} H_i^z S_i^z - 2LJ_2 m_0^2. \tag{2}$$

Here m_0, h are the staggered magnetization and field determined as

$$m_0 = (1/L) \sum_{i=1}^{L} (-1)^i \langle S_i^z \rangle \qquad h^z = -4J_2 m_0$$

in [5, 6]. We modified this approach to take into account the quantum and temperature fluctuations, and the effective field is determined from the spin–spin correlation function:

$$m_0 = (2/L)\sum_{i=1}^{L/2}\sqrt{\mathrm{abs}(S_0^z S_i^z)} \qquad h_i^z = 4J_2\,\mathrm{sgn}(S_i^z)\sqrt{\mathrm{abs}(S_0^z S_i^z)}. \tag{3}$$

Thus we have a one-dimensional antiferromagnet in an effective staggered field h, to be calculated on the basis of a spin–spin correlation function averaged in a MC procedure with 5 MC steps/spin. So a site of the chain (j) is selected using random numbers for every spin configuration in the MC procedure, and the sublattice field is set up starting from this site:

$$h(i-j) \qquad i = j+1, \ldots, j+L/2 \qquad i = j-1, \ldots, j-L/2$$

according to (3). The thermodynamic average of the effective field is a translation-invariant quantity and $\langle h_i^z\rangle = 4J_2 m_0$. Our approach is different from that of [5, 6] while $\langle h_i^2\rangle \neq \langle h_i\rangle^2$.

The algorithm and MC method have been considered in detail earlier [12, 13]. The MC simulations were performed for several lengths of chains $L = 100, 200, 400$ and $m = 32, 64, 96, 124$ with periodic boundary conditions. For each chain, from 4000 to 7000 MC steps per spin were used to reach equilibrium, and another 3000 to 6000 MC steps per spin were used for the averaging. One MC step is achieved by rotating all spins on an $L \times 2m$ lattice. The systematic error due to quantum fluctuations is proportional to $1/(mT/J)^2$ and is of the order of 4% for the minimum temperature $T/J = 0.05$ used in the calculations. The root mean square errors of the computed quantities lie in the ranges 0.1% to 0.6% for the energy, and 6% to 11% for the susceptibility. The errors due to the finite dimensions of the lattice can be neglected, since $\xi < L/4$.

Let us consider the possible spin excitations in this model. There are spin waves (magnons), pair spin excitations, and nonlinear excitations: solitons, kink–antikinks, and breathers (now called spinons). The spinon may be considered as a quasi-particle consisting of bound spins. The phenomenological spinon interpretation is as a domain wall in the 1D antiferromagnetic Ising model. The following quantities will be calculated below: the energy, the specific heat $C = \mathrm{d}E/\mathrm{d}T$, the magnetization, the susceptibility $\chi = M/H$ in an external field, the spin–spin correlation function for the longitudinal $(\langle S^z(0)S^z(r)\rangle)$ and transverse $(\langle S^+(0)S^-(r=1)\rangle)$ spin components, and the Fourier spectrum

$$S(q) = (2/L)\sum_{r=1}^{L/2}\exp(-\mathrm{i}qr)(S_0^z S_r^z).$$

The excitation spectrum can be calculated from imaginary-time quantum Monte Carlo data, where the inherent difficulty of performing inverse Laplace transformations is encountered. In order to overcome this difficulty, a least-squares method [15] and a maximum-entropy method [16] have been proposed. In this report, we do not aim to obtain the dynamical correlation function $S(q, \omega)$ for the whole real-frequency domain, but simply intend to extract the low-lying eigenvalues as a function of q.

Let us introduce an imaginary-time correlation function $S(q, \tau)$ as follows:

$$\begin{aligned} S_t(q,\tau) &= \langle \exp(H\tau)S_q^z \exp(-H\tau)S_{-q}^z\rangle_{MC} \\ S_q^z &= (1/L)\sum_{j=1}^{L} S_j^z \exp(\mathrm{i}qj) \end{aligned} \tag{4}$$

and a two-particle correlation function $S_{s_{1,2}}$, corresponding to the action of two operators $S_j^z S_{j+l}^z$ and $S_j^+ S_{j+l}^-$ on any states—for example, singlet or Néel states:

$$S_j^z S_{j+l}^z |s_j, s_{j+l}\rangle = (1/4)|t_{0,j}t_{0,j+l}\rangle$$

$$(1/2)(S_j^+ S_{j+l}^- + S_j^- S_{j+l}^+)|s_j, s_{j+l}\rangle = (-1/4)(|t_{-1,j}t_{1,j+l} + t_{1,j}t_{-1,j+l}\rangle)$$

where s_j and $t_{0,\pm1,j}$ are respectively called singlet and triplet states with $S^z = 0, \pm1$. The total-system spin does not change under the action of these operators ($\sum_i S_i^z = 0$) and these excitations are of singlet type. One can write $S_{s_{1,2}}$ as

$$S_{s_1}(q,\tau) = \langle \exp(H\tau) S^z_{q,s_1} \exp(-H\tau) S^z_{-q,s_1} \rangle_{MC} \tag{5a}$$

where

$$S^z_{q,s_1} = (1/(L-l)) \sum_{j=1}^{(L-l)/2} [S^z_{2j} S^z_{2j+l} \exp(\mathrm{i}q(2j+l)) + S^z_{2j-1} S^z_{2j+l-1} \exp(\mathrm{i}q(2j+l-1))]$$

and

$$S_{s_2}(q,\tau) = \langle \exp(H\tau) S^{+,-}_{q,s_2} \exp(-H\tau) S^{+,-}_{-q,s_2} \rangle_{MC} \tag{5b}$$

where

$$S^{+,-}_{q,s_2} = (1/2(L-l)) \sum_{j=1}^{(L-l)/2} [(S^+_{2j} S^-_{2j+l} + S^-_{2j} S^+_{2j+l}) \exp(\mathrm{i}q(2j+l)) + (S^+_{2j-1} S^-_{2j+l-1} + S^-_{2j-1} S^+_{2j+l-1}) \exp(\mathrm{i}q(2j+l-1))].$$

Here $\langle \cdots \rangle_{MC}$ denotes a Monte Carlo average of the quantity at a given temperature T, and the momentum changes in the range of $0 < q < \pi$ and is equal to $q = \pi n/(L-l)$, where $n = 0, 1, \ldots, L-l$ and $l = 0, 1, \ldots, 12$. In quantum MC simulations, the imaginary time τ takes a set of discrete numerical values $\tau = \beta n/m$, where $n = 1, 2, \ldots, m$ and $\beta = 1/(k_B T)$. $S_{t,s_i}(q,\tau)$ is obtained by evaluating $S^z_{q,s}$ for two Trotter layers separated by $m/\beta\tau$, $0 < \tau \leqslant \beta/2$, in the transformed two-dimensional Ising system. The spectral function can be approximately represented as

$$S_{t,s}(q,\tau) = \sum_k |\langle \mathrm{GS}|S^z_{q,s}|k,q\rangle|^2 \exp(-\tau(E_{t,s}(q) - E_0)) \tag{6}$$

where the sum is taken over eigenvalues, and $|\mathrm{GS}\rangle$ and E_0 are the ground state and the ground-state energy. Using the nonoverlapping-bands approximation, $|\langle \mathrm{GS}|S^z_q|k,q\rangle|_{k=1}$ is considerably larger than $|\langle \mathrm{GS}|S^z_q|k,q\rangle|_{k\geqslant 2}$, as has been pointed out already [17]; we can extract the elementary excitation spectrum from the Monte Carlo data for $S(q,\tau)$. Three types of function $S_i(q,\tau)$ associated with triplet and singlet excitations are satisfactorily fitted by an exponential dependence on time τ in the range of $\tau_0 < \tau < \tau_{max}$, on the basis of which the dispersion relation is calculated as follows:

$$E_{t,s}(q) = -\ln([S_{t,s}(q,\tau)/S_{t,s}(q,\tau_0)])/(\tau - \tau_0) \tag{7}$$

where $\tau_0 = 1/E_{t,s_i}$ and τ_{max} is close to the onset time for statistical fluctuations in $S(q,\tau)$.

3. Results and discussion

In figure 1 the normalized values of $S_{t,s_{1,2}}(q,\tau)$ are plotted on a logarithmic scale as a function of the distance between the Trotter layers for various values of q and for $T/J_1 = 0.05$, $\lambda = 0.05$. A single-exponential decay of $S(q,\tau)$ is observed, except for the small-τ region. The triplet and singlet excitation spectra are shown in figure 2 for a pure 1D Heisenberg chain for $T/J_1 = 0.05$. The dips near the top of the dispersion curve are due to the deviation of $S(q,\tau)$ from the straight line for small τ. The MC data are well described by the simple form $E_{t,s_{1,2}}(q)/J_1 = A_{t,s}\sin(q)$, where $A_t = 1.63(3)$, $A_s = 1.56(2)$ and indices t, s denote the triplet and singlet excitations. The approximate triplet dispersion relation agrees with the exact result for the one-particle excitations $E_t(q)/J_1 = (\pi/2)\sin(q)$, $0 < q < \pi$ [7]. The two-particle excitation spectrum is split up into two branches of excitations corresponding to $\Delta S^z = 0$ and $\Delta S^z = \pm 1$ by

the action of the staggered field, as shown in figure 3. The singlet ($\Delta S^z = \pm 1$) excitation spectrum exhibits minima at the momenta $q \neq 0, \pi$. These energy minima are associated with a mass gap of Δ_{s_2}.

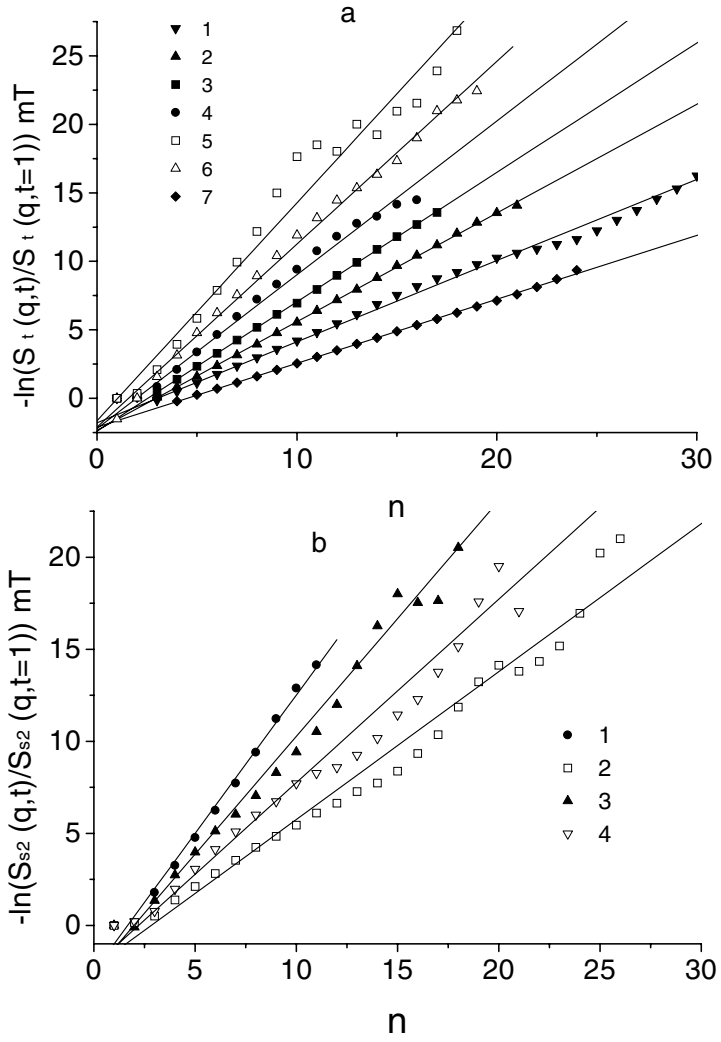

Figure 1. The normalized imaginary-time correlation function $-\ln(S_\alpha(q,t)/S_\alpha(q,t=1))mT$ (where $t = m\tau/\beta$)) for an antiferromagnet versus the distance between the Trotter layers n for $\lambda = 0.05$ and $q = 0.251$ (1), 0.44 (2), 0.565 (3), 0.754 (4), 1.57 (5), 2.7 (6), 3.11 (7) with $\alpha = t$ (a) and $q = 1.57$ (1), 1.63 (3), 1.86 (4), 3.08 (2) with $\alpha = s_2$ (b) for $mT = 4.8$.

The dependence of $E(q)$ can be described by three parameters: the energy maximum E_{max} or the top of the boundary of the spin excitation band, the velocity v, and a gap energy Δ at the centre and at the edges of a band. These parameters were determined by fitting the MC results to the following functions:

$$E(q) = \sqrt{(\Delta^2 + v^2 q^2)} \qquad q < \pi/8$$
$$E(q) = \sqrt{(\Delta^2 + v^2(\pi - q)^2)}.$$

Some of the results are shown in figure 3 by solid lines. The triplet excitation spectrum

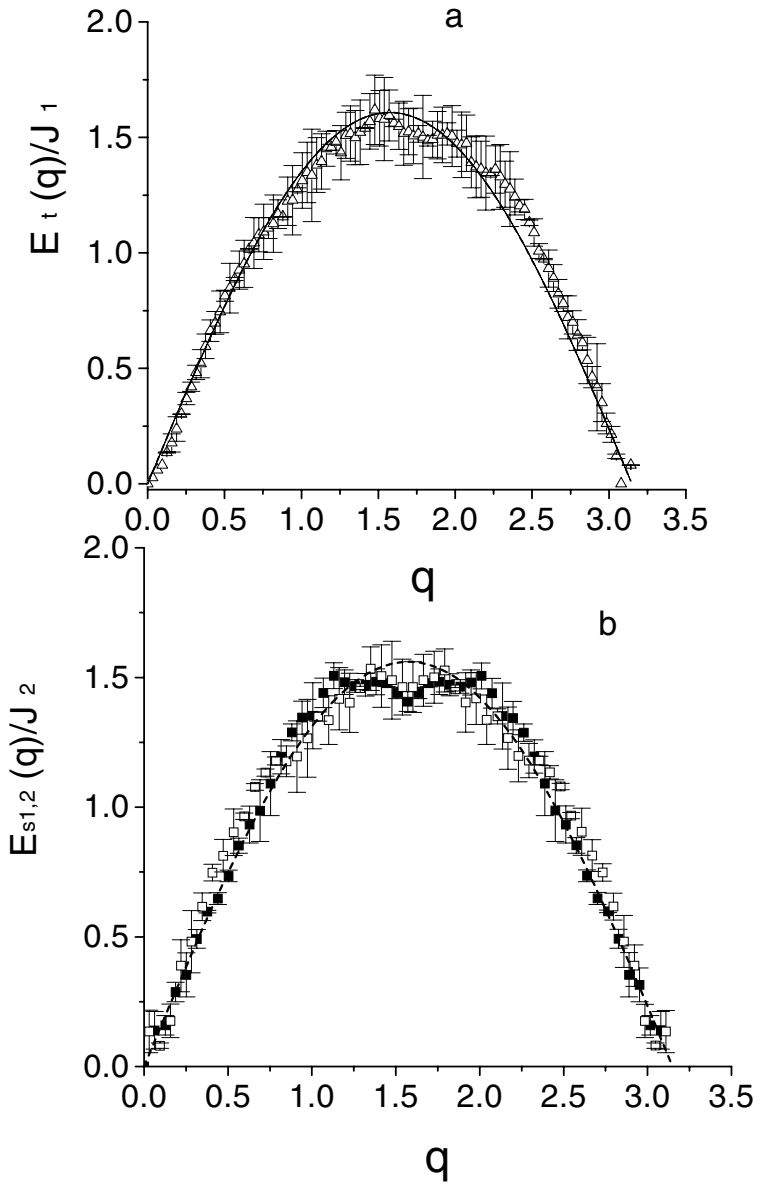

Figure 2. The triplet (a) and singlet (b) excitation spectra of the AF chain ($\lambda = 0$) as functions of the momentum q. The fitting functions are shown by dashed lines: $E_t(q)/J_1 = 1.62\sin(q)$ (a) and $E_{s_{1,2}}/J_1 = 1.56\sin(q)$ (b).

has no symmetry with respect to $q = \pi/2$, the midpoint of the Brillouin zone. The gap is caused by nonlinear excitations at $q = 0$, and is described in terms of spinons. In view of the large error near $q = \pi/2$, the lower limits of the top boundaries of the bands of the triplet and singlet ($\Delta S^z = 0$) excitations are determined and, together with the mass gap at $q = \pi$, are represented in figure 4. $E_{t,s_1,max}$, the lower limit of the energy maximum, fits well on the straight line $E_{t,s_1,max}/J_1 \simeq 1.47(3) + 4.8(3)\lambda$. The Néel temperature of a 3D antiferromagnet is proportional to the energy of the spin-wave band zSJ in the random-phase

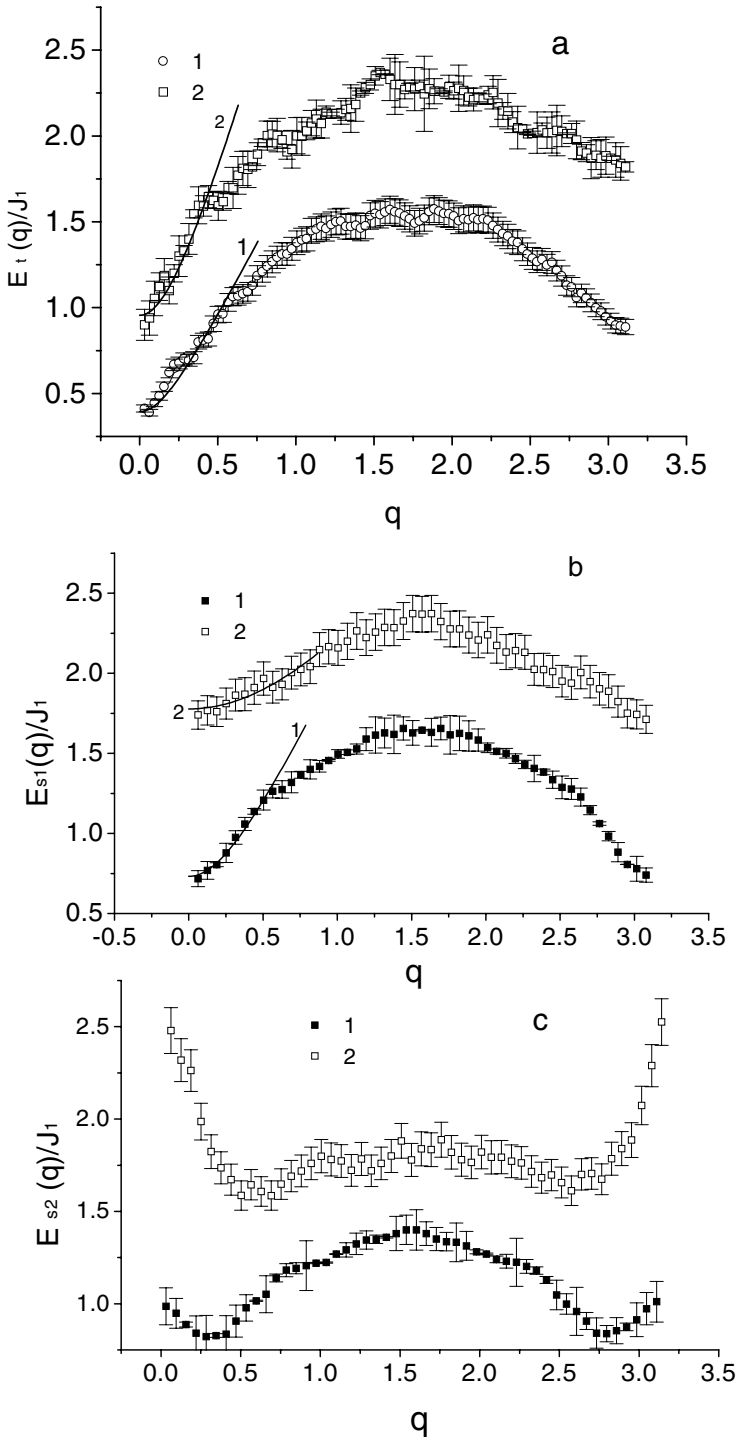

Figure 3. The triplet (a), singlet ($\Delta S^z = 0$) (b), and ($\Delta S^z = \pm 1$) (c) excitation spectra of the antiferromagnet versus the momentum q for $\lambda = 0.05$ (1), 0.2 (2). The fitting functions are $E_t/J_1 = \sqrt{([0.36(5)]^2 + [1.75(4)]^2 q^2)}$ (1), $E_t/J_1 = \sqrt{([0.95(2)]^2 + [1.92(8)]^2 q^2)}$ (2), $E_{s_1}/J_1 = \sqrt{([0.73(2)]^2 + [1.91(4)]^2 q^2)}$ (1), $E_{s_1}/J_1 = \sqrt{([1.76(7)]^2 + [1.3(6)]^2 q^2)}$ (2).

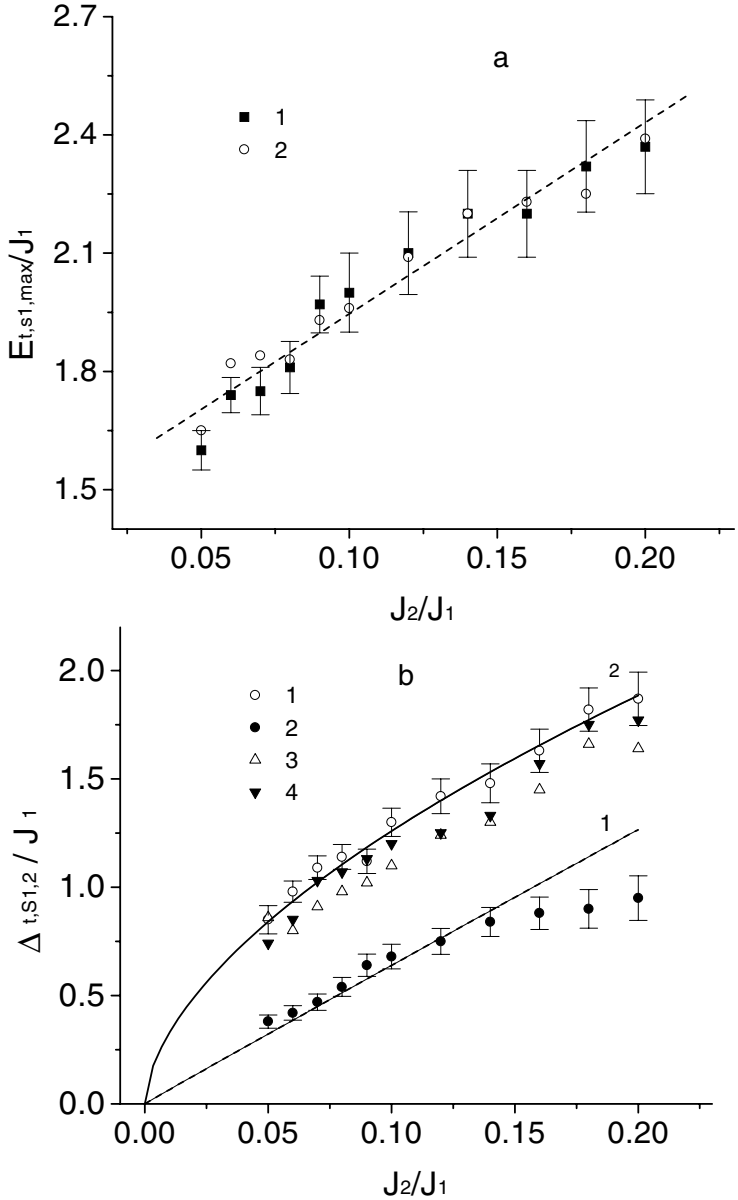

Figure 4. (a) The lower limits of the top boundaries in the triplet (1) and singlet ($\Delta S^z = 0$) (2) excitation spectra versus the normalized interchain coupling J_2/J_1. The fitting function is the straight line $E_t/J_1 = 1.47(3) + 4.8(3)\lambda$. (b) The gap energies as functions of λ for the triplet, at $q = \pi$ (1) and $q = 0$ (2), and the singlet, with $\Delta S^z = 0$ (4) and $\Delta S^z = \pm 1$ (3) excitations. The fitting functions are $\Delta_{sp}/J_1 = 6.2(2)\lambda$ with $\lambda < 0.15$ (1: dashed line) and $\Delta_t/J_1 = 4.8(3)\lambda^{0.58(3)}$ (2: full line).

approximation. Below, we shall show that the dependence $T_N(\lambda)$ on the interchain coupling is similar to $E_{t,s_1,max}(\lambda)$. The values of the triplet gap at $q = 0$ are approximated by a straight line, $\Delta_{sp}/J_1 = 6.2(2)\lambda$, for $\lambda < 1/8$, and agree well with the exact solution for a fermionic model of a one-dimensional antiferromagnet in an effective staggered field, derived on the

basis of the approximation of the continuum limit and constant couplings [5] $\Delta \simeq 6.175|J_2|$, as illustrated in figure 4(b). The triplet gap is parametrized at $q = \pi$ as $\Delta_t/J_1 = 4.8(3)\lambda^{0.58(3)}$. A similar power law characterizes the singlet gap, $\Delta_s(\lambda)$. The singlet gaps are independent of the distance between two spins in the triplet:

$$\cdots \uparrow \underbrace{\cdots}_{l} \downarrow \cdots \uparrow \underbrace{\cdots}_{l} \downarrow \qquad (\Delta S^z = 0)$$

or

$$\cdots \uparrow \underbrace{\cdots}_{l} \uparrow \cdots \downarrow \underbrace{\cdots}_{l} \downarrow \qquad (\Delta S^z = \pm 1)$$

since the mean-field approximation is used. The gaps in the triplet excitation spectrum at the $(q = 0)$ centre and at the $(q = \pi)$ boundary of the zone disappear at some critical temperatures T_1 and T_2, as plotted in figure 5(a). The magnitude of T_2 is determined from a fit of the MC results to the function $\Delta_t/J_1 = A((T - T_2)/J_1)^\beta$ with three parameters A, β, T_2, where β is varied in the range of 0.4–0.6. The line approximations $T_1/J_1 = 0.9(1)\lambda$ and $T_2/J_1 = 1.5(2)\lambda$ are obtained from the five points for $\lambda \leqslant 1/8$. The gap closure in the singlet excitation spectrum $(\Delta S^z = 0)$ occurs in the vicinity of temperature T_2, and the $\Delta S^z = \pm 1$ excitation becomes massless at $T > T_2$ (see figure 5(b)).

The external magnetic field produces an effect also on the singlet and triplet excitation spectra. The excitation spectra of the one-dimensional AF in the staggered field are shown for different external fields at low temperatures in figure 6. The asymmetry of the triplet excitation spectrum is due to the different quasi-particles. So the gaps in the excitation spectra are attributable to spinons at $q = 0$ and magnons at $q = \pi$. They are closed respectively at the external fields H_{c1} and H_{c2}, as illustrated in figure 7(a). The minima in the singlet $\Delta S^z = \pm 1$ excitation spectrum are revealed at $q = 0, \pi$ for $H > H_{c1}$. When the average of the staggered field tends to zero, the spin excitation spectrum is similar to the spectrum of a one-dimensional chain, and $E_{max,t}/J_1 \sim \pi/2$. The singlet excitation spectrum becomes massless at $H > H_{c2}$ as shown in figure 7(b).

Now we shall consider the static magnetic properties of the AF in the staggered-field model and interpret some distinctive behaviours of the temperature and field as regards the thermodynamic characteristics. Long-range order exists in the staggered field and breaks down at the Néel temperature T_N, which can be determined from the disappearance of the staggered magnetization, $\sigma \to 0$, plotted in figure 8(a). The staggered magnetization and the susceptibility are quite independent of temperature for low temperatures $T < T_1$ and $\chi \to 0$ as shown in figure 9(b). The greatest variations of the longitudinal component of the square of the total spin, $\langle (S^z)^2 \rangle$, versus temperature are revealed at the temperatures T_1 and T_2 shown in figure 8(b). The absolute value of the nearest-spin correlation functions exhibits a sharp decrease and the specific heat has an additional maximum in the vicinity of $T \simeq T_1$ shown in figure 9(a). These effects can be caused by spinon excitations, the density of which shows a sharp rise upon closure of the gap in the triplet excitation spectrum at the Brillouin zone centre. From fit of the temperature dependence of $C(T)$ with the function $C(T)/k_B N = A(T/J_1)^\alpha \exp(-\Delta/T)$ with three parameters A, α, Δ, a satisfactory agreement of the Δ value is obtained with the gap in the spinon excitation spectrum. For example, the fitting function $C(T)/k_B N = 0.3/(T/J_1)^{2.0(2)} \exp(-0.61(6)J_1/T)$ plotted in the inset of figure 9 for $\lambda = 0.1$ gives the gap value $\Delta/J_1 = 0.61(6)$, which agrees well with the exact result $\Delta_{sp}/J_1 = 0.6175$ [5].

The temperature dependence of the susceptibility exhibits a 'crevasse' in the curve for $T > T_2$ (figure 9(b)), which is due to a rise of the density of states of the singlet excitations occurring because $\Delta_{s_{1,2}} \to 0$ at $T \simeq T_2$. The existence of a gap in the triplet excitation

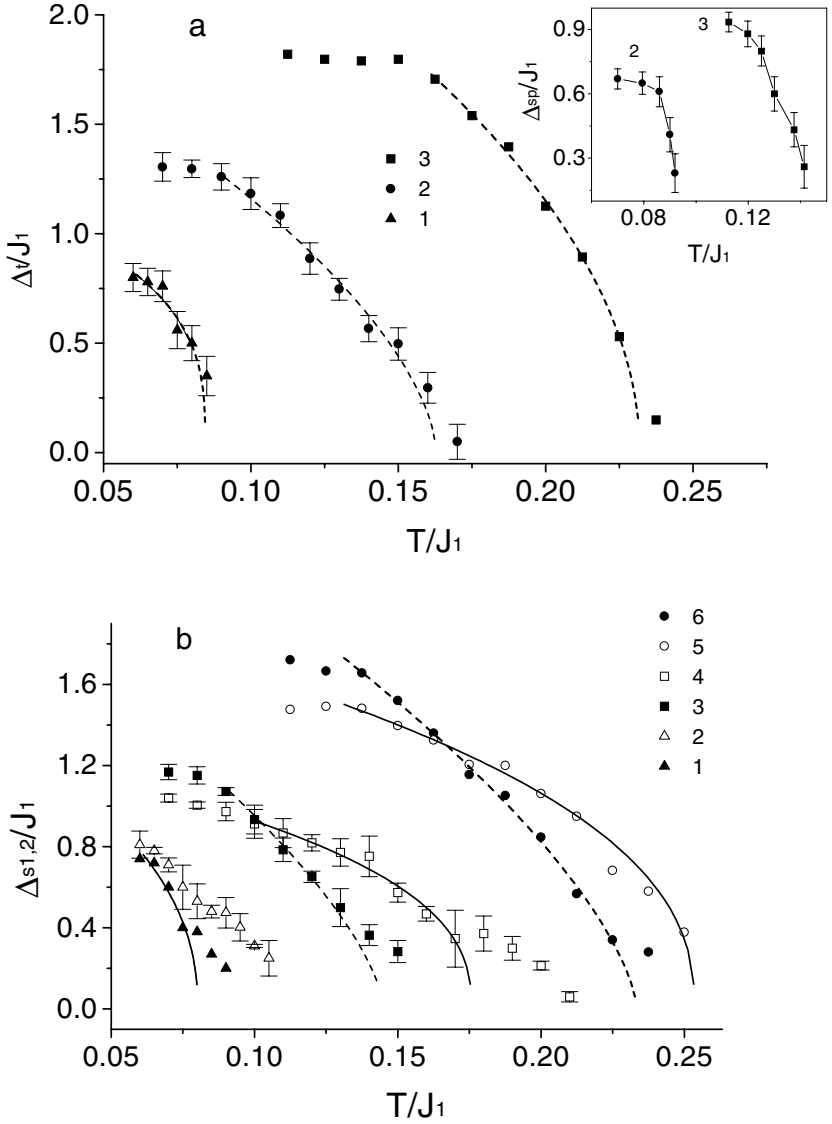

Figure 5. The gap energies Δ_α in the triplet excitation spectrum for $\alpha = t$, $\lambda = 0.05$ (1), 0.1 (2), 0.2 (3) at $q = \pi$ (a) and the singlet excitation spectrum for $\alpha = s_1$ (1, 3, 6), s_2 (2, 4, 5), $\lambda = 0.05$ (1, 2), 0.1 (3, 4), 0.2 (5, 6) (b) against temperature. The fitting functions $\Delta/J_1 = A((T - T_{1,2})/J_1)^\beta$ are plotted as solid and dashed lines. The temperature dependencies of the triplet gaps at $q = 0$ for $\lambda = 0.1$ (2), 0.2 (3) are shown in the inset.

spectrum is confirmed by the field dependence of the magnetization plotted in figure 10. For $T < T_1$, the magnetization is equal to zero down to the critical field H_c, at which the staggered magnetization decreases sharply and the total magnetization exhibits a jump. These discontinuities of the first kind pass into gradual continuous dependencies of $M(H)$, $\sigma(H)$ for $T > T_1$. The critical fields calculated fit well on the straight line $H_c/J_1 = (3.8 \pm 0.3)\lambda$ over the range of $0.05 \leqslant \lambda \leqslant 0.15$.

The Néel temperatures and the staggered magnetizations determined for the temperature

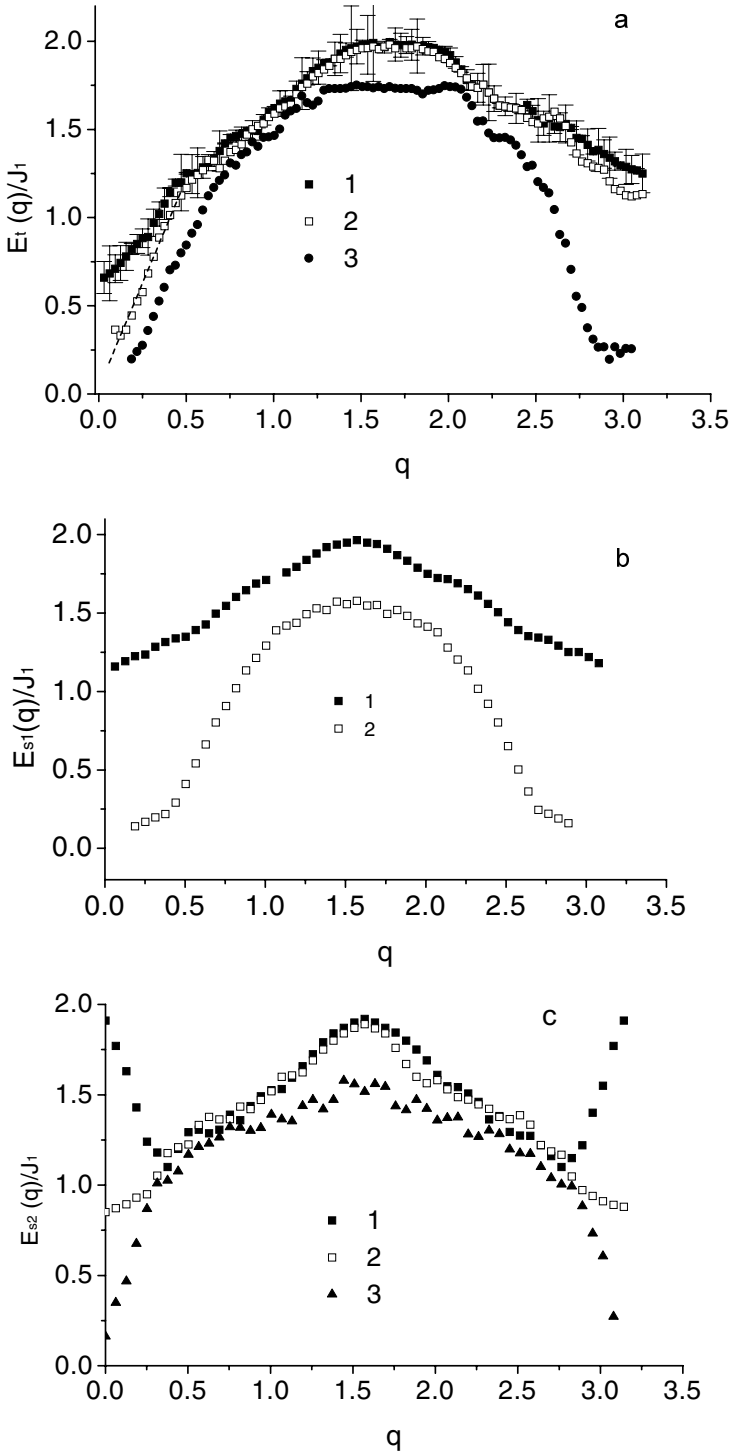

Figure 6. The spectra $E_\alpha(q)$ of the triplet excitations with $\alpha = t$, $H/J_1 = 0.05$ (1), 0.15 (2), 0.35 (3) (a), and singlet excitations with $\alpha = s_1$, $H/J_1 = 0.05$ (1), 0.35 (2) (b) and $\alpha = s_2$, $H/J_1 = 0.05$ (1), 0.15 (2), 0.4 (c) for various magnetic fields as functions of the momentum q.

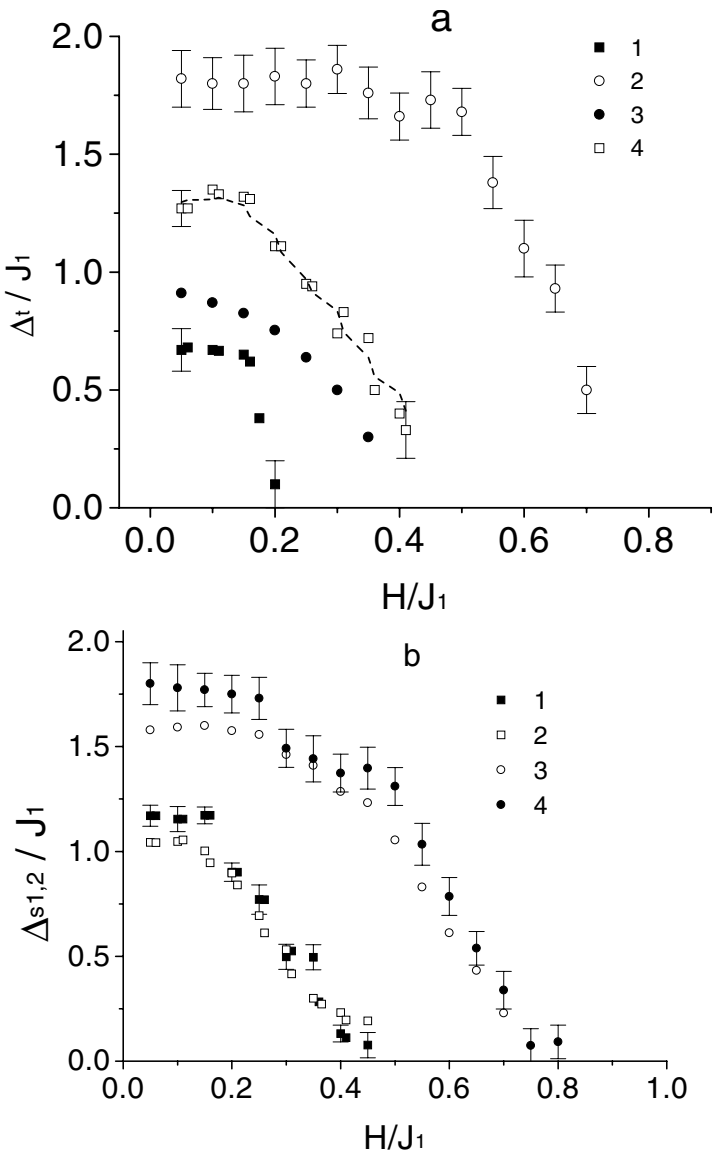

Figure 7. The gap energies Δ_α in the triplet excitation spectrum with $\alpha = t$, $\lambda = 0.1$ (1, 2), 0.2 (3, 4) for $q = \pi$ (2, 3), $q = 0$ (1, 4) (a) and the singlet excitation spectrum with $\alpha = s_1$ (1, 4), s_2 (2, 3), $\lambda = 0.1$ (1, 2), 0.2 (3, 4) (b) against the external magnetic field H/J_1.

range of (0.15–0.25)T_N are plotted in figure 11. For comparison, we show predictions for $T_N(\lambda)$ and $\sigma(\lambda)$ from the spin-wave theory with kinematic interactions (marked 'SW') [3] and the chain mean-field theory (marked 'CMF') [5]. The spin-wave theory predicts $T_N/J_1 = 2.1S(S+1)\sqrt{\lambda}$, $\sigma \approx 1/\ln(1/\lambda)$ [3] and the chain mean-field theory leads to $T_N/J_1 \sim \lambda$, $\sigma \sim \sqrt{\lambda}$ up to logarithmic corrections. The MC results are in good agreement with the chain mean-field results for $\lambda \leqslant 1/8$. This means that the spinon excitations provide the main contribution to the spin excitation density for weakly coupled chains.

Now we will apply our results for interpretation and to predict new effects for the low-

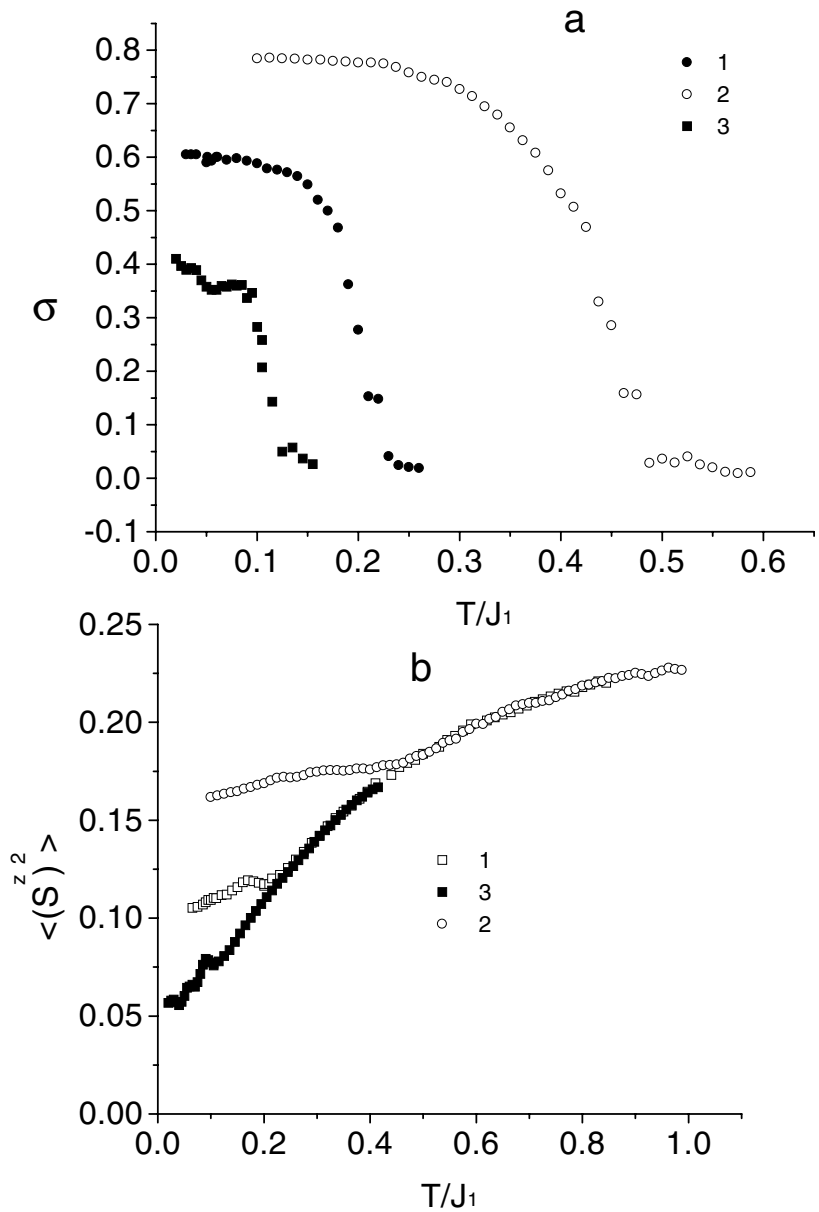

Figure 8. The staggered magnetization σ (a) and the longitudinal component of the square of the total spin, $\langle (S^z)^2 \rangle$, (b) as functions of the temperature for $\lambda = 0.05$ (3), 0.1 (1), 0.25 (2).

dimensional magnets. From an inelastic neutron scattering experiment, the intrachain exchange is estimated as $J_1 = 203$ K in $KCuF_3$ [8]. The intrachain exchange interaction for Sr_2CuO_3 as estimated from the fit of the magnetic susceptibility [20] to theoretical calculations using conformal field theory is $J_E = 2200(200)$ K [22] and the numerical estimate for the finite-length chain is $J_B = 2800$ K [18]. The Néel temperatures are $T_N \approx 39$ K for $KCuF_3$ [9], $T_N \approx 5.4$ K for Sr_2CuO_3, and $T_N \approx 11$ K for Ca_2CuO_3 [10]. From the MC simulations of the Néel temperature and the staggered magnetization, the intrachain and interchain couplings

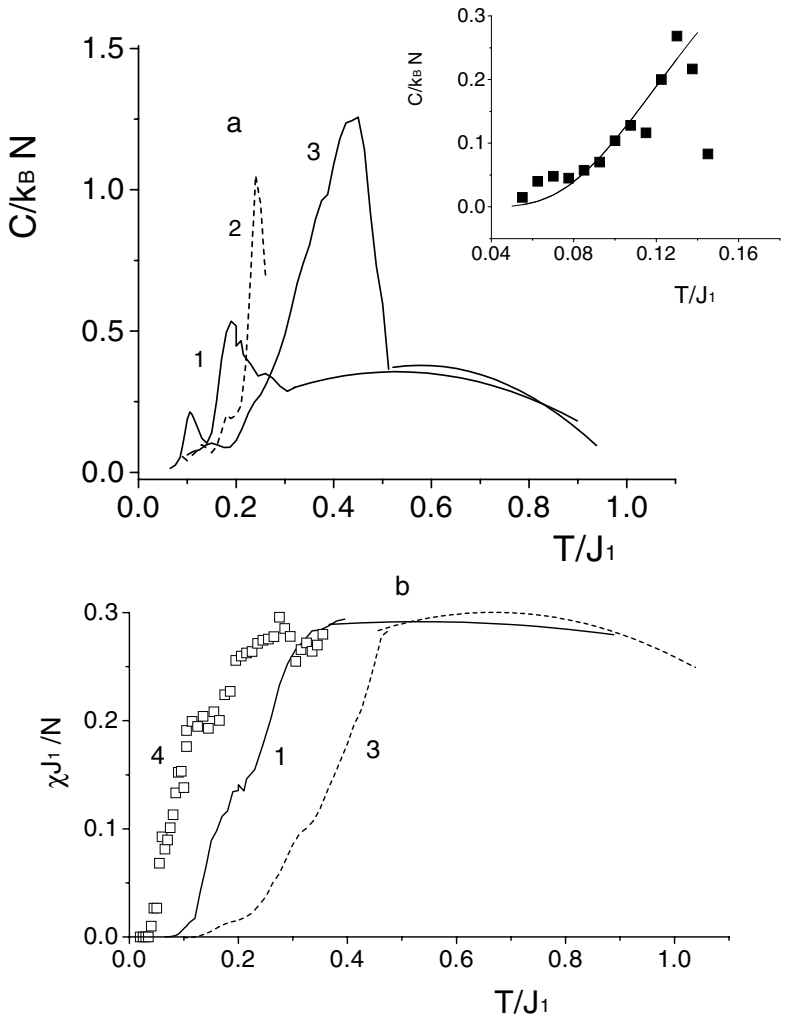

Figure 9. The specific heat $C/(k_BN)$ (a) and the susceptibility $\chi J_1/N$ (b) of the AF as functions of the temperature for $\lambda = 0.05$ (4), 0.1 (1), 0.15 (2), 0.25 (3). The inset shows the fitting function $C(T)/(k_BN) = 0.3/(T/J_1)^2 \exp(-0.61(6)J_1/T)$ (solid line) for $\lambda = 0.1$.

and the magnetic moment at a site are determined as $J_2 \approx 20$ K, $\sigma \approx 0.6\ \mu_B$ for $KCuF_3$, $J_1 \approx 2840$ K, $J_2 \approx 2.8$ K, $\sigma \simeq 0.06\ \mu_B$ for Sr_2CuO_3, and $J_1 \approx 2209$ K, $J_2 \approx 5$ K, $\sigma \simeq 0.09\ \mu_B$ for Ca_2CuO_3. The predicted value of the staggered magnetization exceeds the experimental result $\sigma = 0.5\ \mu_B$ for $KCuF_3$ [19] and is in good agreement with $\sigma = 0.06(3)\ \mu_B$ for Sr_2CuO_3 [10] and $\sigma = 0.09(1)\ \mu_B$ for Ca_2CuO_3 [10, 11]. The overestimation of the magnetization may be attributed to spin–phonon interaction which causes the additional spin reduction. It is of interest to note that the ground state of the similar compound $KCuCl_3$ [21] is the singlet state. The intrachain coupling estimated for Sr_2CuO_3 matches well with $J_B = 2800$ K determined by Bonner–Fisher theory [18].

The sharp rise in the energy-dependent neutron scattering intensity observed around $\omega = 10$ meV [9] for $KCuF_3$ can be attributed to the interaction between the neutrons and the spinons excitation at $\omega^{MC} = 10.6$ meV. From the estimated singlet excitation spectrum,

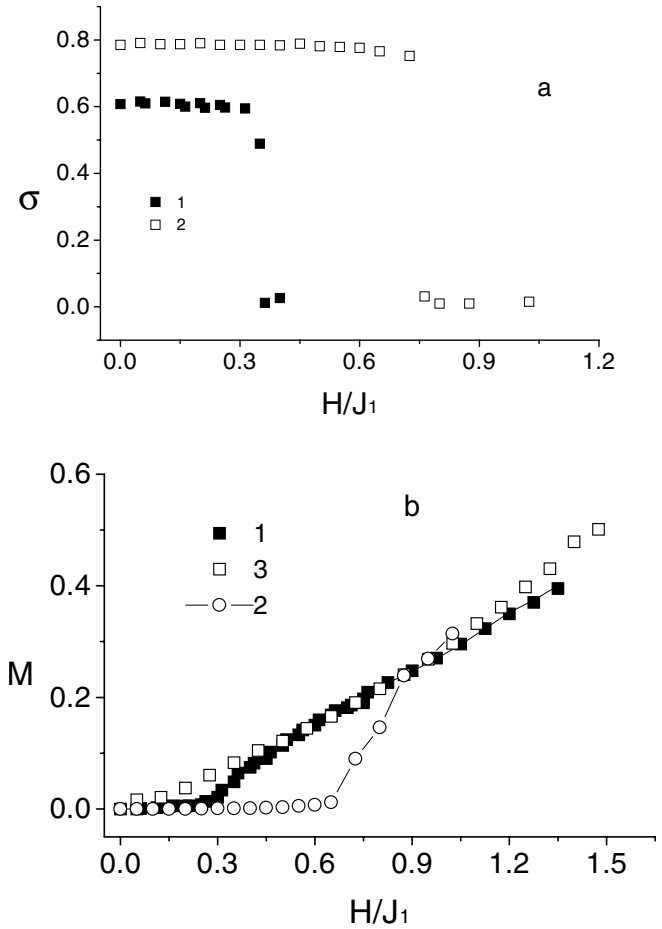

Figure 10. The field dependencies of the staggered magnetization σ (a) and the magnetization M (b) for $\lambda = 0.1$ (1, 3), 0.25 (2) at $T = T_N/4$ (1, 2) and at $T = 0.65T_N$ (3).

nontrivial predictions are given for the singlet gap energy at $\omega_s(0, 0, \pi) \simeq 19$ meV for $KCuF_3$, which can be obtained from observation by means of light scattering and from the linewidth of the AF resonance. The decrease of the integrated intensities of the magnetic Bragg reflections within the limits $\sim$12% at $T \approx 3.5$ K for Sr_2CuO_3 and the decreasing local field at the muon sites within $\sim$15% at $T \simeq 7$ K are due to the closure of the gap in the spin excitation spectrum at $T_2^{MC} \simeq 4.3$ K for Sr_2CuO_3 and at $T_2^{MC} \simeq 8.3$ K for Ca_2CuO_3. The mass gaps in the singlet excitation spectra are determined to lie at $\omega_s(0, 1/2, 1/2) \simeq 22$ meV for Ca_2CuO_3 and at $\omega_s(0, 1/2, 1/2) \simeq 17$ meV for Sr_2CuO_3.

Summarizing our results, we have determined the energies of the gaps in the spectra of triplet and singlet excitations for weakly coupled AF chains. The spinon gap disappears at the critical temperature $T_1/J_1 = 0.9\lambda$; the triplet gap at $q = \pi$ is at the critical magnetic field $H_c/J_1 = 3.8\lambda$ and the singlet gaps are closed at $T_2/J_1 = 1.5\lambda$. At these temperatures, the staggered magnetization, the specific heat, and the spin–spin correlation functions exhibit some distinctive behaviours. The mass gaps in the triplet and singlet two-particle excitation spectra are predicted for $KCuF_3$, Sr_2CuO_3, and Ca_2CuO_3. The neutron scattering at $\omega = 10$ meV in $KCuF_3$ is successfully explained, as is the inflection point of the staggered magnetization

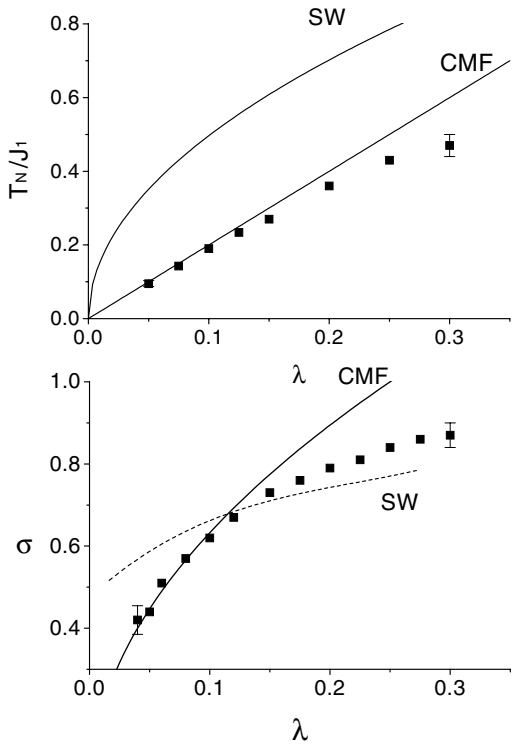

Figure 11. The Néel temperature T_N/J_1 and the staggered magnetization σ as functions of $\lambda = J_2/J_1$. The MC results are denoted by squares. The spin-wave theory with kinematic interactions is marked 'SW' [3] and the chain mean-field theory is marked 'CMF' [5].

at $T \simeq 0.65T_N$ for Sr_2CuO_3 and Ca_2CuO_3. The validity of the MC results is demonstrated by the good agreement of the Néel temperature, the staggered magnetization, and the spinon mass gap with results from general scaling arguments.

Acknowledgment

The paper was supported by grant INTAS-97 12124.

References

[1] Parola A, Sorella S and Zhong Q F 1993 *Phys. Rev. Lett.* **71** 4393
[2] Affleck I, Gelfand M P and Singh R P 1994 *J. Phys. A: Math. Gen.* **27** 7313
[3] Welz D 1993 *J. Phys.: Condens. Matter* **5** 3643
[4] Schulz H J and Bourbonnais C 1983 *Phys. Rev.* B **27** 5856
[5] Schulz H J 1996 *Phys. Rev. Lett.* **77** 2790
[6] Scalapino D J, Imry Y and Pincus P 1975 *Phys. Rev.* B **11** 2042
[7] Faddeev L D and Takhtajan L A 1981 *Phys. Lett.* A **85** 375
[8] Satija S K *et al* 1980 *Phys. Rev.* B **21** 2001
[9] Tennant D A *et al* 1995 *Phys. Rev.* B **52** 13 381
[10] Kojima K M, Fudamoto Y and Larkin M 1997 *Phys. Rev. Lett.* **78** 1787
[11] Yamada K *et al* 1995 *Physica* C **253** 135
[12] Raedt H and Lagendijk A 1985 *Phys. Rep.* **127** 233
[13] Aplesnin S S 1996 *Phys. Solid State* **38** 1031

[14] Suzuki M 1986 *J. Stat. Phys.* **43** 883
[15] White S R, Scalapino D J, Sugar R L and Bickers N E 1989 *Phys. Rev. Lett.* **63** 1523
[16] Sivia D S and Gubernatis J E 1990 *Phys. Rev.* B **41** 380
[17] Takahashi M 1993 *Phys. Rev.* B **48** 311
[18] Bonner J C and Fisher M E 1964 *Phys. Rev.* **135** A640
[19] Hutchings M T *et al* 1969 *Phys. Rev.* **188** 919
[20] Motoyama N, Eisaki H and Uchida S 1996 *Phys. Rev. Lett.* **76** 3212
[21] Kato T, Takatsu K and Tanaka H 1998 *J. Phys. Soc. Japan* **67** 752
[22] Eggert S, Affleck I and Takahashi M 1994 *Phys. Rev. Lett.* **73** 332